

Final Report to



COMPOSITION VARIATION DURING FLOW OF GAS-CONDENSATE WELLS

Project Number 07122-29.FINAL

September 2011

Authors: Hai Xuan Vo and Roland N.
Horne

PI: Roland N. Horne (horne@stanford.edu)
Department of Energy Resources Engineering
367 Panama Street
Stanford University, CA 94305-2220
(650)723-4744

LEGAL NOTICE

This report was prepared by Stanford University as an account of work sponsored by the Research Partnership to Secure Energy for America, RPSEA. Neither RPSEA members of RPSEA, the National Energy Technology Laboratory, the U.S. Department of Energy, nor any person acting on behalf of any of the entities:

- a. MAKES ANY WARRANTY OR REPRESENTATION, EXPRESS OR IMPLIED WITH RESPECT TO ACCURACY, COMPLETENESS, OR USEFULNESS OF THE INFORMATION CONTAINED IN THIS DOCUMENT, OR THAT THE USE OF ANY INFORMATION, APPARATUS, METHOD, OR PROCESS DISCLOSED IN THIS DOCUMENT MAY NOT INFRINGE PRIVATELY OWNED RIGHTS, OR
- b. ASSUMES ANY LIABILITY WITH RESPECT TO THE USE OF, OR FOR ANY AND ALL DAMAGES RESULTING FROM THE USE OF, ANY INFORMATION, APPARATUS, METHOD, OR PROCESS DISCLOSED IN THIS DOCUMENT.

THIS IS A FINAL REPORT. THE DATA, CALCULATIONS, INFORMATION, CONCLUSIONS, AND/OR RECOMMENDATIONS REPORTED HEREIN ARE THE PROPERTY OF THE U.S. DEPARTMENT OF ENERGY.

REFERENCE TO TRADE NAMES OR SPECIFIC COMMERCIAL PRODUCTS, COMMODITIES, OR SERVICES IN THIS REPORT DOES NOT REPRESENT OR CONSTITUTE AND ENDORSEMENT, RECOMMENDATION, OR FAVORING BY RPSEA OR ITS CONTRACTORS OF THE SPECIFIC COMMERCIAL PRODUCT, COMMODITY, OR SERVICE.

Signature Page

A handwritten signature in blue ink, appearing to read "Roland N. Horne". The signature is fluid and cursive, with the first name "Roland" being more prominent than the last name "Horne".

Roland N. Horne, Principal Investigator

5 December 2011

Abstract

Gas-condensate wells experience a significant decrease in gas productivity once the flowing bottom-hole pressure drops below the dew-point pressure. However, there is still a lack of understanding how the condensate bank affects the deliverability because of the complex phase and flow behaviors. The difficulty of understanding the phase and flow behaviors lies in the variation of the composition due to the existence of two-phase flow and the relative permeability effect (each phase has different mobility). The change of composition will also bring about a large change in saturation and phase properties such as surface tension, viscosity, etc. of the fluids. These effects will impact mobilities and hence productivity.

The composition variation has been observed in the field but its effects have been studied only rarely in the literature. This work studied the impact of compositional variation on the flow behavior of the gas-condensate system through numerical simulations and a series of laboratory experiments. The study verified claims made about effect of flow through porous media on the apparent phase behavior of a gas-condensate mixture, namely compositional variation during depletion, saturation profile around the well, experience on shutting in the wells in an attempt to achieve condensate revaporization, and the effect of bottom-hole pressures on condensate banking.

Results from this study show that composition varies significantly during depletion. Due to the difference in mobilities caused by relative permeability, the composition of the mixture will change locally. The overall composition near the wellbore becomes richer in heavy components. As a result, the phase envelope will shift to the right. Near-well fluids can undergo a transition from retrograde gas to a volatile oil, passing through a critical composition in the process. The condensate bank can be reduced with proper producing sequence, hence the productivity of the well can be improved, for example by raising the bottomhole flowing pressure.

Finally, the study investigated the effect of compositional variation on the optimization of the producing strategy for gas-condensate reservoirs, reducing the impact of condensate banking, and improving the ultimate gas and condensate recovery. Conducting an optimization calculation using Genetic Algorithm, an example reservoir was used to determine the optimal production strategy to benefit from the understanding of composition change during production. This same approach can be applied to real producing reservoirs, by substituting the real reservoir configuration in the numerical simulation model.

Contents

Abstract	v
Contents	vii
List of Figures	ix
1. Introduction	3
1.1. Overview	3
1.2. Scope of this Work.....	5
2. Experimental Investigation	7
2.1. Experimental Design.....	7
2.1.1. Synthetic Gas-Condensate Mixture	7
2.2. Experimental Apparatus.....	9
2.2.1. Computerized Tomography (CT) Scanner.....	9
2.3. Experimental Procedures	10
2.3.1. Gas-condensate Core Flooding Experiments	10
2.3.2. Gas-condensate, Immobile Water Core Flooding Experiments.....	12
2.3.3. Compositional Measurement	13
2.3.4. Saturation Measurement	13
2.4. Results	14
2.4.1. Gas-Condensate Flow without Water	14
2.4.2. Gas-Condensate with Immobile Water	20
2.5. Saturation	20
3. Impact to Producers	23
3.1. Optimization of Revenue from Gas-Condensate Reservoirs	23
4. Conclusion	29
References	31

List of Figures

Figure 1-1: Phase diagram of a typical gas condensate with line of isothermal reduction of reservoir pressure.	3
Figure 1-2: Illustration of pressure profile and liquid dropout in the near wellbore region.	4
Figure 1-3: An example of very poor performance of a gas-condensate well (from Barnum et al., 1995).....	5
Figure 2-1: Phase diagram of the synthetic gas-condensate mixture used for experiments (85% C_1 and 15% nC_4 in mole fraction).....	8
Figure 2-2: Condensate dropout of the synthetic gas-condensate mixture used for experiments (85% C_1 and 15% nC_4 in mole fraction) at 70 °F from the simulation of CCE and CVD tests.....	8
Figure 2-3: Modified experiment apparatus to minimize sample tube volume.	9
Figure 2-4: GE HiSpeed CT/i.	10
Figure 2-5: Performing experiments in the CT scanning room.	13
Figure 2-6: Gas-condensate noncapture experiment 1: nC_4 in the flowing mixture.....	15
Figure 2-7: Gas-condensate noncapture experiment 2: nC_4 in the flowing mixture.....	15
Figure 2-8: Gas-condensate noncapture experiment 3: nC_4 in the flowing mixture.....	16
Figure 2-9: Gas-condensate noncapture experiment: nC_4 in the flowing mixture with different BHP control cases.	17
Figure 2-10: Condensate revaporization after noncapture experiment for gas-condensate system 1.....	17
Figure 2-11: Condensate revaporization after noncapture experiment for gas-condensate system 2.....	18
Figure 2-12: Condensate revaporization after noncapture experiment for gas-condensate system 3.....	18
Figure 2-13: Gas-condensate capture experiment 1.....	19

Figure 2-14: Gas-condensate capture experiment 2.....	19
Figure 2-15: Gas-condensate capture experiment 3.....	20
Figure 2-16: Gas-condensate-immobile water noncapture experiment 1: nC_4 in the flowing mixture.....	21
Figure 2-17: Gas-condensate-immobile water noncapture experiment 2: nC_4 in the flowing mixture.....	21
Figure 2-18: Gas-condensate noncapture experiment 3: (a) nC_4 in the flowing phases. (b) condensate saturation profile.	22
Figure 3-1: The SPE3 reservoir model (Kenyon and Behie, 1987).	23
Figure 3-2: Phase diagram of the gas-condensate reservoir fluid.	24
Figure 3-3: Gas injection rate of the optimization problem.....	25
Figure 3-4: Revenue of an example gas-condensate reservoir under different injection rate scenarios.....	26
Figure 3-5: Cumulative condensate production of the optimization problem.	26
Figure 3-6: Cumulative gas production of the optimization problem.....	27
Figure 3-7: Cumulative gas injection of the optimization problem.	27
Figure 3-8: Condensate to gas production ratio of the optimization problem.	28

Executive Summary

One of the most significant and unique factors associated with tight gas reservoirs is their low productivity, which is especially exacerbated in the case of gas-condensate fluids. Gas-condensates fluids exhibit complex phase and flow behaviors due to the appearance of condensate banking in the near-well region, and differ essentially in their behavior from conventional gas reservoirs, especially for low permeability high yield condensate systems, which have more severe condensate banking problems. A good understanding of how the condensate accumulation influences the productivity and the composition configuration in the liquid phase is very important to optimize the producing strategy for tight gas sands, to reduce the impact of condensate banking, and to improve the ultimate gas recovery.

This study addressed several issues related to the behavior of the composition variation, condensate saturation build-up and condensate recovery during the gas-condensate producing process in tight gas reservoirs. A key factor that controls the gas-condensate well deliverability is the relative permeability, which is influenced directly by the condensate accumulation. The accumulated condensate bank not only reduces both the gas and liquid relative permeability, but also changes the phase composition of the reservoir fluid, hence reshapes the phase diagram of reservoir fluid and varies the fluid properties. The study found that different producing strategies impact the composition configuration for both flowing and static phases and the amount of the liquid trapped in the reservoir, which in turn influence the well productivity and hence the ultimate gas and liquid recovery from the reservoir. Changing the manner in which the well is brought into flowing condition was found to affect the liquid dropout composition and can therefore change the degree of productivity loss.

Experiments using a binary synthetic mixture at laboratory scale were conducted to measure the compositional variation and to test the contributing factors for composition variation and condensate banking effect. Full compositional simulations of binary-component and multicomponent gas-condensate fluids were conducted at field scale to investigate the composition and condensate saturation variations. Different producing strategies were tested to find out the optimum producing sequences for maximum gas recovery. By taking account of the new understanding of the impact of compositional changes, the composition of the liquid dropout can be “controlled” by the production strategy (for example by dropping a lighter liquid in preference to a heavier one) and hence the recovery from tight gas reservoirs with condensate fluids can be improved.

As a primary result, it was determined that increasing the bottomhole flowing pressure of wells producing gas-condensate fluids can (depending on the composition) result in a more valuable flow stream (in terms of net present value, NPV). One important consequence of the composition variation examined in this work is that the reservoir fluid progressively changes from a gas condensate to a volatile oil because the heavier components are left in the formation due to relative permeability effects. This means that

producing companies are not able to revaporize the condensate by repressurizing the wells.

Another way for producing companies to improve the productivity by adjusting the compositional behavior of the reservoir fluid is to inject lean gas, for example by partial gas recycling.

This report includes an abbreviated summary of the results and conclusions – a more complete compilation of the experimental and numerical procedures and results is contained in an accompanying Appendix report.

1. Introduction

1.1. Overview

Gas-condensate reservoirs are encountered more frequently as exploration is now targeted at greater depth and hence higher pressure and temperature. The high temperature and pressure lead to a higher degree of degradation of complex organic molecules. As a result, the deeper the burial of an organic material, the higher tendency the organic material will be converted to gas or gas condensate. The gas condensate usually consists mainly of methane and other light hydrocarbons with a small portion of heavier components.

Gas condensate has a phase diagram as in Figure 1-1. In this case, the reservoir temperature lies between the critical temperature and the cricondentherm, the maximum temperature at which two phases can coexist in equilibrium. Initially, the reservoir pressure is at a point that is above the dew-point curve so the reservoir is in the gaseous state only. During production, the pressure declines isothermally from the reservoir boundary to the well. If the well flowing bottom-hole pressure (*BHP*) drops below the dew-point pressure, the condensate drops out of the gas and forms a bank of liquid around the well (Figure 1-2). The gas condensate is special in the sense that when the pressure decreases isothermally, instead of having gas evolution from liquid, we have liquid condensation from the gas. Hence, sometimes, gas condensate is also called “retrograde gas”.

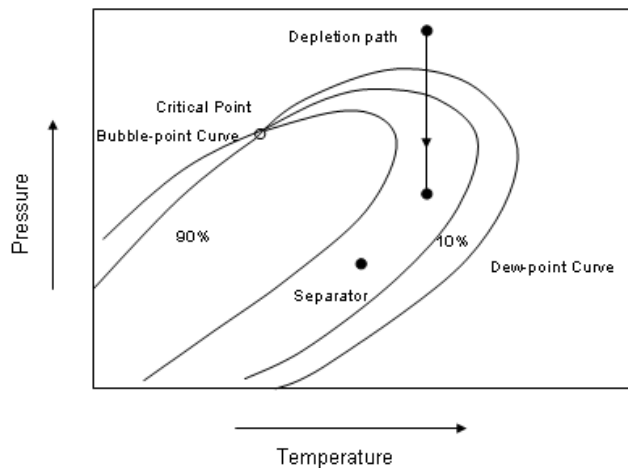


Figure 1-1: Phase diagram of a typical gas condensate with line of isothermal reduction of reservoir pressure.

When the condensate drops out in the reservoir, at first, due to relative permeability behavior, the condensate liquid will not flow until the accumulated condensate saturation exceeds the critical condensate saturation. This leads to a loss of valuable hydrocarbons because the condensate contains most of the heavy components. Besides that, near the

wellbore where the condensate bank appears, there will be a multiphase flow so the gas relative permeability is reduced. The reduction of gas permeability due to the condensate bank is called condensate blocking. The condensate blocking effect leads to a reduction of gas productivity of the well.

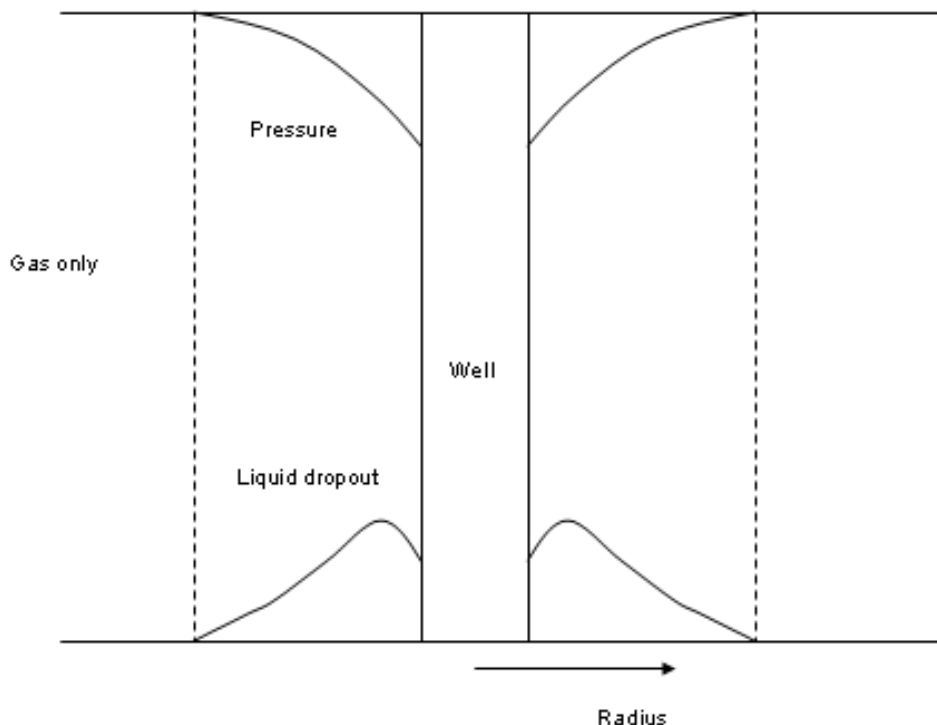


Figure 1-2: Illustration of pressure profile and liquid dropout in the near wellbore region.

The productivity loss due to condensate build up is large in some cases, especially in tight reservoirs. Afidick et al. (1994) reported that liquid accumulation had occurred around the wellbore in the Arun field and that it had reduced individual well productivity by 50% even though the retrograde-liquid condensation in laboratory *PVT* experiments was less than 2%. Barnum et al. (1995) conducted a study using data from 17 fields and concluded that the condensation of hydrocarbon liquids in gas-condensate reservoirs can restrict gas productivity severely. However, gas recovery factors below 50% are limited to reservoirs with a permeability-thickness less than 1,000 md-ft. For more permeable reservoirs, the productivity loss is not as severe. Barnum et al. (1995) also presented one example of poor well performance (Figure 1-3). This is a moderately rich gas-condensate field with an initial condensate-gas ratio of 73 bbl/MMscf. The well produced at initial rates over 1 MMscf/day. When the flowing bottom-hole pressure reached the dew-point, gas production declined rapidly and the well died. Pressure surveys indicated that the well was full of liquid hydrocarbons. Attempts to swab the well were unsuccessful, even though data from surrounding wells indicated the average reservoir pressure was still over 2,000 psi above the dew-point pressure. The well appeared to have “locked up” and ceased production shortly after flowing bottom-hole pressure fell below the dew-point pressure. Eventually the well was stimulated successfully by hydraulic fracturing, and it returned to the initial production rates.

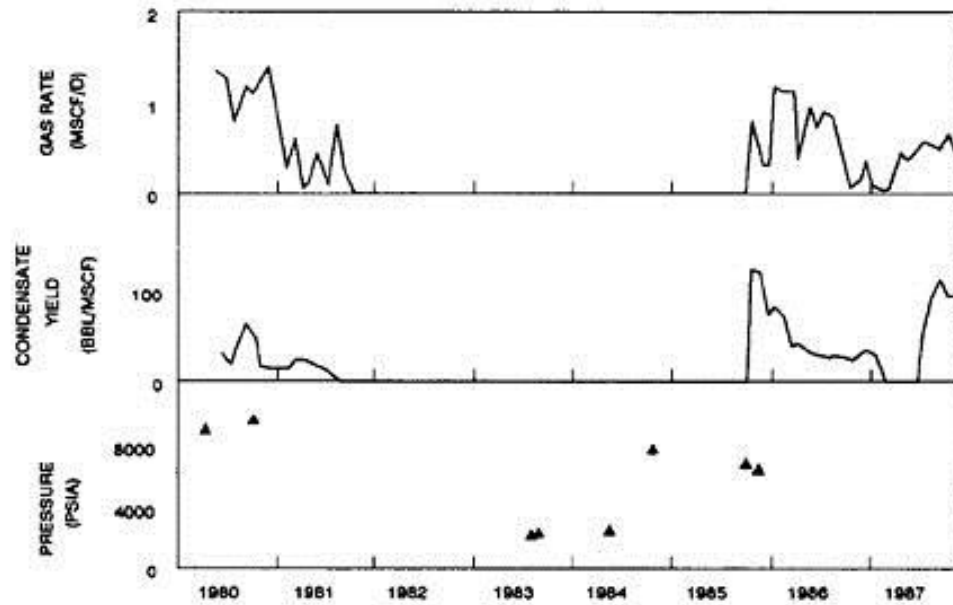


Figure 1-3: An example of very poor performance of a gas-condensate well (from Barnum et al., 1995).

1.2. Scope of this Work

The focus of the research was to gain a better understanding of how condensate blocking affects the well productivity, with a focus on the effect of compositional variation on flow behavior. This is important for optimizing the performance of gas-condensate reservoirs, reducing the impact of condensate banking, and improving the ultimate gas and condensate recovery.

The objective of the project was to develop methodology to increase the productivity of gas-condensate fluids from tight gas reservoirs in the US. Presently, gas-condensate reservoirs experience reductions in productivity by as much as a factor of 10 due to the dropout of liquid close to the wellbore. The reduction is worse in low permeability formations that make up tight gas reservoirs. The liquid dropout blocks the flow of gas to the well and lowers the overall energy output by a very substantial degree (90% if the productivity is reduced by 10). The combination of condensate phase behavior and rock relative permeability results in a change of composition of the reservoir fluid, as heavier components separate into the dropped-out liquid while the flowing gas phase becomes lighter in composition. This effect has been sparsely recognized in the literature, although there is clear evidence of it in field observations. The project quantified the effect, developed a scientific understanding of the phenomena, and used the results to investigate ways to enhance the productivity by controlling the liquid composition that drops out close to the well. By optimizing the producing pressure strategy, it was found to be possible to cause a lighter liquid to be condensed in the reservoir, after which the productivity loss would be more easily remedied.

The research made use of experimental measurements of gas-condensate flow, as well as compositional numerical simulations. The following issues and their contribution to

condensate banking and composition changes in tight gas reservoirs were examined carefully:

1. How does the reservoir permeability contribute to the condensate banking problem? How can understanding of this effect be used to reduce the production loss in low permeability gas-condensate systems?
2. How do the reservoir flow properties (PVT, rich or lean gas-condensate system) and phase behavior play a role in composition change and how can we predict the component change given a flow characterization?
3. How does the composition change relate to the production sequence? Can we design a production strategy for tight gas reservoirs that will apply different producing schemes to maximize the gas recovery?

2. Experimental Investigation

2.1. Experimental Design

The strategy was to use a simple binary mixture in the experiments. Although field gases have more complex composition, the use of a binary mixture in the laboratory improved the ability to achieve accurate results. The laboratory results obtained using the binary mixture could then be used subsequently to confirm numerical simulation results with the same composition, then finally the numerical simulator was used with more complex compositions found in the field.

2.1.1. *Synthetic Gas-Condensate Mixture*

The binary mixture used in the experiments was 85% C_1 and 15% nC_4 by mole fraction. This gas-condensate mixture was selected based on the following criteria:

- The binary mixture is easy to mix in the laboratory, from commercial high quality pure component gases.
- The critical temperature of the mixture is below the laboratory temperature so the experiments can be performed at room temperature, which eliminates the need to heat the flammable gases hence improving safety.
- The gas has a broad two-phase region in order to achieve condensate dropout during the experiment.

The phase diagram of the synthetic gas-condensate mixture used for the experiments is shown in Figure 2-1. The critical point of the mixture is $T_c = 10^\circ\text{F}$, $p_c = 1,844$ psia. At room temperature of 70°F and pressure range from 2,200 – 1,000 psia, this mixture has a broad two-phase region.

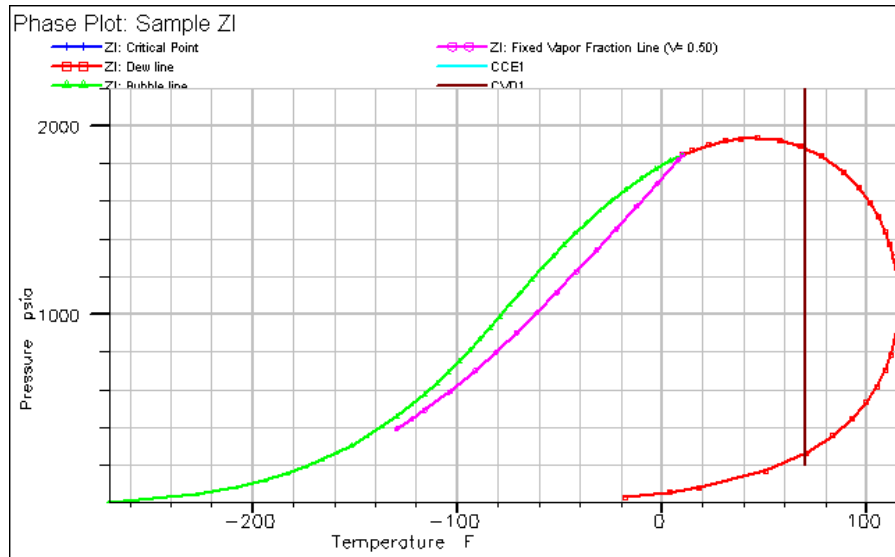


Figure 2-1: Phase diagram of the synthetic gas-condensate mixture used for experiments (85% C_1 and 15% nC_4 in mole fraction).

Figure 2-2 shows the condensate dropout volumes in *CVD* and *CCE* tests. The accumulated condensate volumes from both tests are almost the same in the condensing region. Both tests also show that the condensate revaporizes into the gas phase at lower pressure. These static PVT tests do not account for the condensate buildup hence they do not indicate the maximum possible condensate accumulation in the reservoir. The maximum liquid dropout volumes from these simple PVT tests are less than 12%. However, as we found from reservoir simulation, the condensate saturation during actual flow can be as high as 47% due to relative permeability effects.

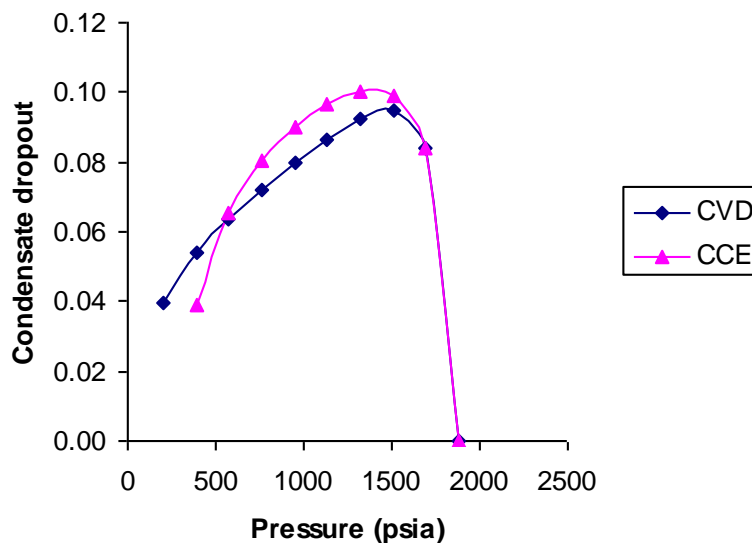


Figure 2-2: Condensate dropout of the synthetic gas-condensate mixture used for experiments (85% C_1 and 15% nC_4 in mole fraction) at 70 °F from the simulation of *CCE* and *CVD* tests.

The core used in the experiments is a low permeability sandstone. The synthetic gas-condensate mixture was injected at one end and produced at the other end of the core, so the flow was one-dimensional linear flow.

Numerical simulations were conducted to define the experimental parameters. Simulation was also used to check the flow pressures and to have an idea how composition and saturation were distributed along the core. In the simulation model, two wells, one gas injection and one producing, were used. Both wells were controlled by constant bottom-hole pressures. The bottom-hole pressure of the injection well was set above the dew-point pressure while the bottom-hole pressure of the producing well was set below the dew-point pressure of the gas-condensate mixture. So the fluid at the upstream end was always in gas phase, and the fluid at the downstream end was always in the two-phase region.

2.2. Experimental Apparatus

The apparatus was modified from a previous design of Shi (Shi, 2009) to achieve repeatability of the experimental results. The apparatus was modified by fitting valves directly onto the core holder to minimize the volume in the sample tubes. The modification is shown in Figure 2-3. The modified experimental apparatus consists of the three main subsystems: gas supply and exhaust, core flooding system and fluid sampling system.

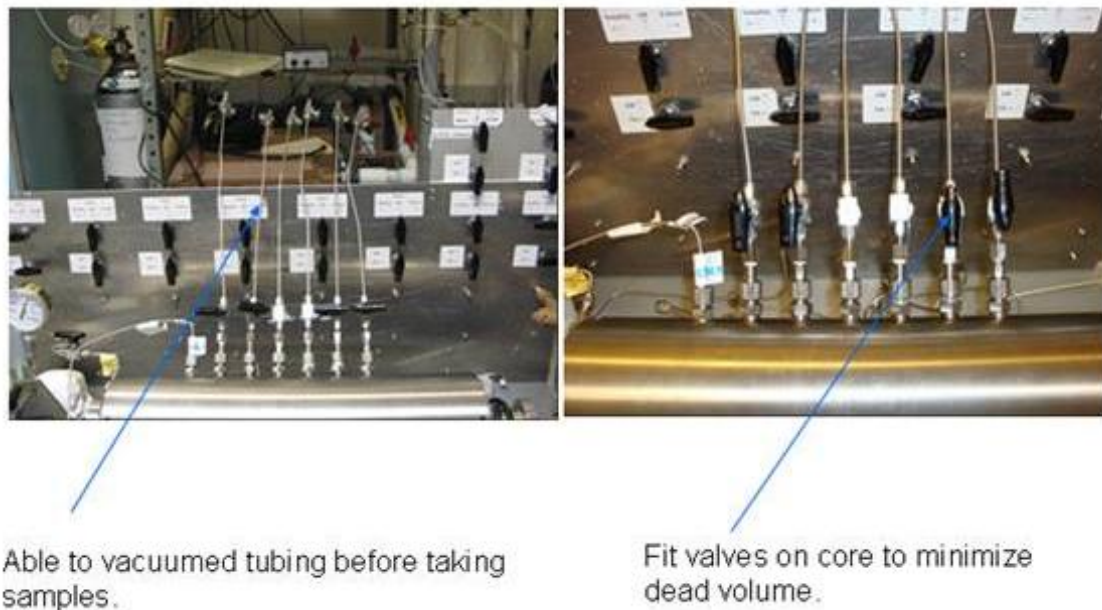


Figure 2-3: Modified experiment apparatus to minimize sample tube volume.

2.2.1. Computerized Tomography (CT) Scanner

In this study, a GE HiSpeed CT/i scanner was used to measure the saturation distribution along the core during the experiments (Figure 2-4). For two-phase systems and three-

phase systems where the third phase is immobile, a single energy level scan is sufficient to determine the saturations.



Figure 2-4: GE HiSpeed CT/i.

2.3. Experimental Procedures

2.3.1. Gas-condensate Core Flooding Experiments

Two types of experiments were performed in this study: noncapture and capture. The difference between them was that in the noncapture experiments the samples were taken while the fluid was flowing, while in the capture experiments fluid flowed through the core for a given time period then both inlet and outlet valves were closed at the same time. The samples were then taken from the “captured” fluid. At the end, the remaining fluid in the core was discharged to an empty cylinder to determine the composition of the condensate left in the core. These experimental procedures were modified from the previous procedures to achieve repeatability of the results.

Noncapture Experiments

In the noncapture experiment, the whole system was vacuumed overnight and the core was presaturated with C_1 at 2,200 psi. The gas-condensate cylinder was compressed to 2,200 psi (dew-point pressure of the 85%-15% moles C_1 - nC_4 is around 1,840 psi) using nitrogen pushing on the back of the piston inside the cylinder. The gas-condensate mixture was then flushed through the core to displace C_1 with the downstream pressure at 2,000 psi (about 160 psi above the dew-point pressure of the gas mixture).

The first step of the procedure was to inject C_1 directly into the vacuumed core. This was done to make sure that the gas mixture was in the gaseous state in the core and we could flush the gas mixture through to core to displace methane without dropping below the dew-point pressure of the gas mixture. The C_1 - nC_4 mixture was flushed through the core for 10 minutes. Then the downstream valve was closed, and the core contents sampled through the sample tubes. The first five batches of samples were discarded to eliminate all residual methane in the dead volumes of the sampling ports. The sample tubings were vacuumed and samples were taken under no-flow conditions. After demonstrating good repeatability under no-flow conditions, the sample tubings were vacuumed again. The gas-condensate mixture was flushed through the core at 1,000 psi differential pressure for 3 minutes, and flow samples were taken. Both upstream and downstream valves were then closed. To avoid artifacts in X-ray CT images, the sample tubings were removed before scanning. The plastic handles of the valves on the core holder were also removed. The core was then scanned in the X-ray CT scanner to determine the saturation distribution.

The compositional behavior under different well flowing bottom-hole pressure (*BHP*) control was then investigated using the noncapture experiments. The experimental procedure was to keep the same upstream pressure but vary the downstream pressure and measure the composition corresponding to each downstream pressure. The core could also be scanned to determine the saturation distribution.

Finally, we studied the effect of repressurization on revaporization of the condensate. Due to the relative permeability effect and difference in mobilities of the gas and condensate phases, the overall in-situ composition changes thereby shifting the phase envelope of the gas condensate. In this case, shutting in a well may not be a good strategy because the condensate may not revaporize back to gas. The procedure of the repressurization experiment was to first perform all the steps for the noncapture experiment. After taking the flow samples, we shut the downstream valve and let the pressure in the core build up to 2,200 psi. After 35 minutes, samples along the core were taken. The saturation distribution was also determined by *CT* scanning. This procedure mimics the real situation in which a well is producing in a gas-condensate reservoir: after the *BHP* drops below the dew-point pressure, and the well is shut in in an attempt to achieve condensate revaporization.

Capture Experiments

Capture experiments were designed to have flow samples under conditions in which both upstream and downstream valves were closed so the samples would be closer to static composition rather than that of the flowing gas. Furthermore, the captured condensate in the core could be discharged to an empty cylinder to determine the composition of the condensate dropout.

The whole system was vacuumed overnight and the core was presaturated with C_1 at 2,200 psi. The original procedure had been to presaturate with C_1 at 2,000 psi. The gas-condensate cylinder was compressed to 2,200 psi (dew-point pressure of 85%-15% molar C_1 - nC_4 is around 1,840 psi) using nitrogen pushing on the back of the piston inside the cylinder. The gas-condensate mixture was flushed through the core for 10 minutes with the downstream pressure at 2,000 psi (about 160 psi above the dew-point pressure of the gas mixture). This was done to make sure that the gas mixture was in the gaseous state at the inlet of the core and we could flush the gas mixture through to core to displace methane without dropping below the dew-point pressure of the gas mixture (original procedure was at 2,000 – 1,950 psi differential pressure so it had been difficult to remove the methane out of the core). The C_1 - nC_4 mixture was flushed through the core for 10 minutes. Then the downstream valve was closed and the fluids sampled. The first five batches of samples were discarded to eliminate all residual methane in the dead volumes of the sampling ports. The sample tubings were vacuumed and samples were taken under no-flow conditions.

After demonstrating good repeatability under no-flow conditions, the sample tubings were vacuumed and the gas-condensate mixture was flowed through the core at 1,000 psi differential pressure for 3 minutes. Then the upstream and downstream valves were closed simultaneously. Fluid samples were taken in capture mode immediately. At the end, the entire content of the core was discharged into an empty (vacuumed) cylinder for compositional analysis.

After scanning the core during noncapture experiments, we found out that the titanium core-holder had caused X-ray beam hardening which can affect the measurement results for saturation. We decided not to use the CT scanner for subsequent experiments.

2.3.2. Gas-condensate, Immobile Water Core Flooding Experiments

The core holder was vacuumed for 48 hours if there was some water in the core previously. The vacuum pump was connected at the outlet of the core holder, the inlet valve was closed. After that, the water pump was connected to the inlet of the core holder. The inlet valve was opened. Deionized water was pumped in while keeping the vacuum pump on. The vacuum pump was turned off and disconnected when water reached the tubing at the outlet. The estimated time was calculated based on the water pumping rate and the pore volume. Water pumping was continued to displace about four pore volumes to eliminate any air trapped in the core. The upstream of the core holder was then lifted to an angle about 30 degrees from horizontal. C_1 was injected through the core at 50-100 psi

for two to three hours to drain the water to immobile water saturation S_{wi} . The sample tubings were also bled off from time to time to release trapped water. The core holder was then put back to the horizontal position, the downstream valve was closed and the core was filled with C_1 at 2,200 psi. The capture and noncapture experiments were performed in the same way as for the previous gas-condensate system without water. No *CT* scanning was used for the gas-condensate-immobile water experiments.

2.3.3. Compositional Measurement

The gas samples that needed to be analyzed were collected in Tedlar gas sample bags. The bag can be connected directly to the *GC* for analysis. A T-connector was used to vacuum the whole system before injecting the sample into the *GC* in order to protect the sample from being contaminated by air. For each gas sample, at least two runs through the *GC* were conducted to make sure the result was consistent. It was also noticed that to have good results the *GC* needs to be conditioned regularly to remove residuals on the detectors. This involves baking the *GC* at high temperature for a given period and calibrating the *GC* again, as outlined in the user manual.

2.3.4. Saturation Measurement

Measurements with the X-ray *CT* scanner are subject to a variety of errors and image artifacts including positioning error, beam hardening, object shape, and obstruction.

Positioning error was eliminated in this study by fixing the core holder on the table of the *CT* scanner and performing all scans without moving it, as shown in Figure 2-5.



Figure 2-5: Performing experiments in the *CT* scanning room.

The X-ray source of the *CT* scanner delivers a spectrum of X-ray energies rather than single-level energy. The lower energies are absorbed in the core holder, rock and at the interfaces. Beam hardening is the process of increasing the average energy level of an X-ray beam by filtering out the low-energy photons. This creates an error in the linear attenuation measurement. In analyzing the rock, beam hardening can be reduced by using special core holder designs (surrounding the core holder with a cylindrical water jacket, using an aluminum core holder, etc.), moving to higher energy levels or calibrating the *CT* scanner to a *CT* number higher than that of water using a doped water solution. In this study, we tried to minimize the beam hardening by using higher energy level (140 kV).

2.4. Results

2.4.1. Gas-Condensate Flow without Water

Noncapture Experiments

The compositional distribution along the core during a gas-condensate noncapture experiment is shown in Figure 2-6. No-flow samples were taken before the flow test when the gas mixture was above the dew-point. The no-flow compositions were repeated perfectly and were identical to the composition from the source cylinder. This confirmation indicated that the rock does not have an effect on the (static) phase behavior of the gas mixture.

During flow through the core, going from left to right, the pressure drop was higher. Liquid dropped out in the core and accumulated in the rock. The flowing mixture became lighter (more C_1) and the concentration of nC_4 in the flowing phase along the core decreased.

Figure 2-7 and Figure 2-8 show two more noncapture experiments following the same procedure. The compositional distributions along the core confirm the result in Figure 2-6. These results also confirm the three-region theory and the simulations results.

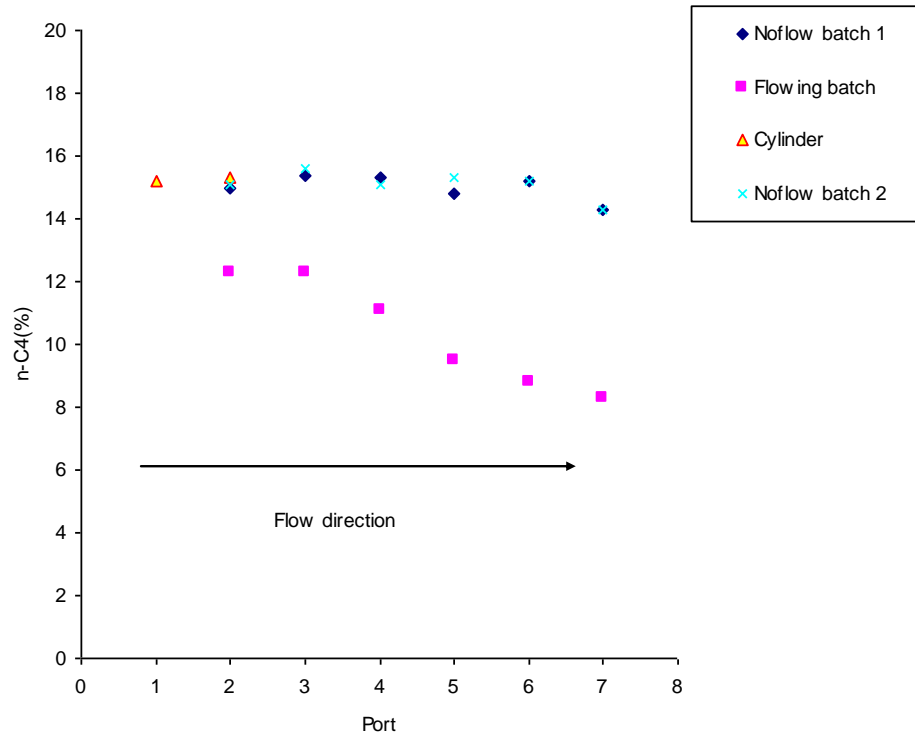


Figure 2-6: Gas-condensate noncapture experiment 1: $n\text{C}_4$ in the flowing mixture.

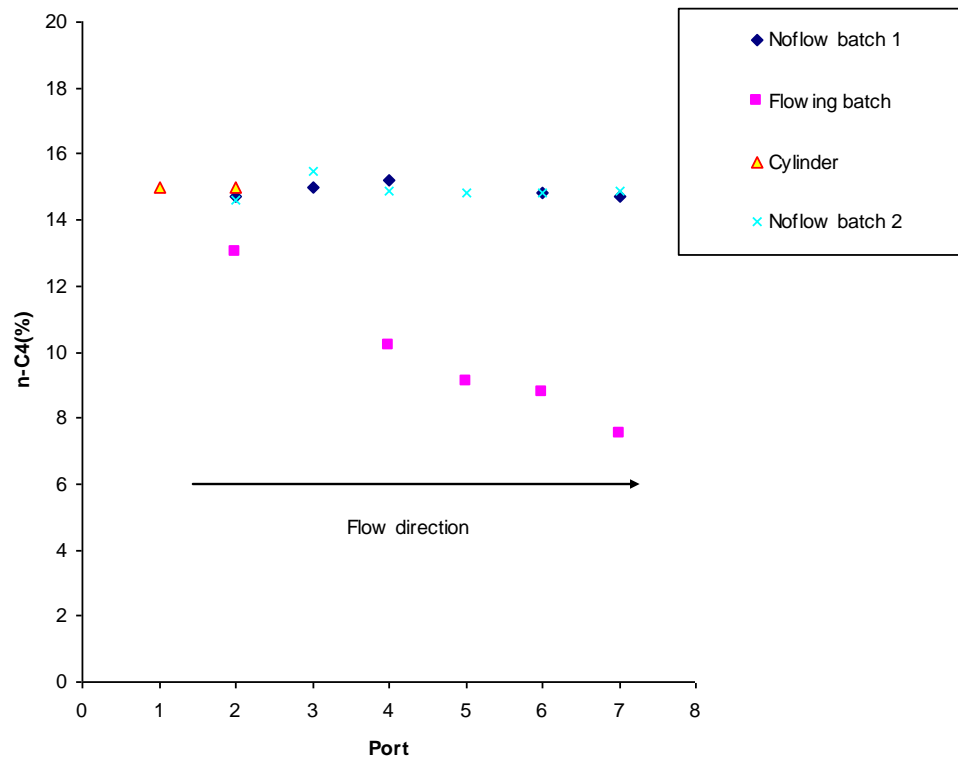


Figure 2-7: Gas-condensate noncapture experiment 2: $n\text{C}_4$ in the flowing mixture.

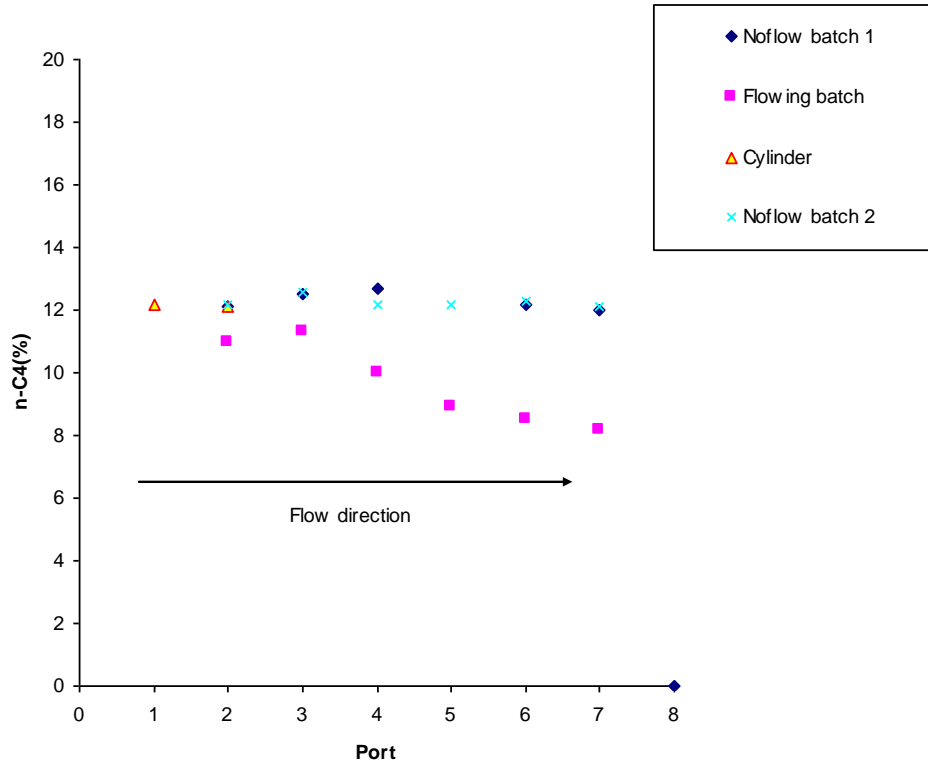


Figure 2-8: Gas-condensate noncapture experiment 3: nC_4 in the flowing mixture.

The effect of producing pressure (BHP in a real well) on the composition is shown in Figure 2-9. The result in Figure 2-9 shows that the higher the pressure drop below the dew-point the more nC_4 accumulates in the condensate, and the less nC_4 is found in the flowing mixture. This experimental result confirms the simulation result reported previously by Shi (2009). This finding is important because it tells us a way to minimize the condensate banking by minimizing the pressure drop below the dew-point by either producing the well at higher pressure or applying partial pressure maintenance (using gas cycling for example).

The results of revaporization experiments are shown in Figure 2-10 to Figure 2-12 in three different experiments. In the first experiment (Figure 2-10), composition during flow was not registered. However in the other two experiments (Figure 2-11 and Figure 2-12) it is clear that the composition changes after flow stops, but not all the way back to the original gas composition. Hence we can see that after 35 minutes the condensate does not revaporize fully back into gas. This confirms the shift of the phase envelope and hence that shutting the well is not an effective strategy to remove the condensate bank.

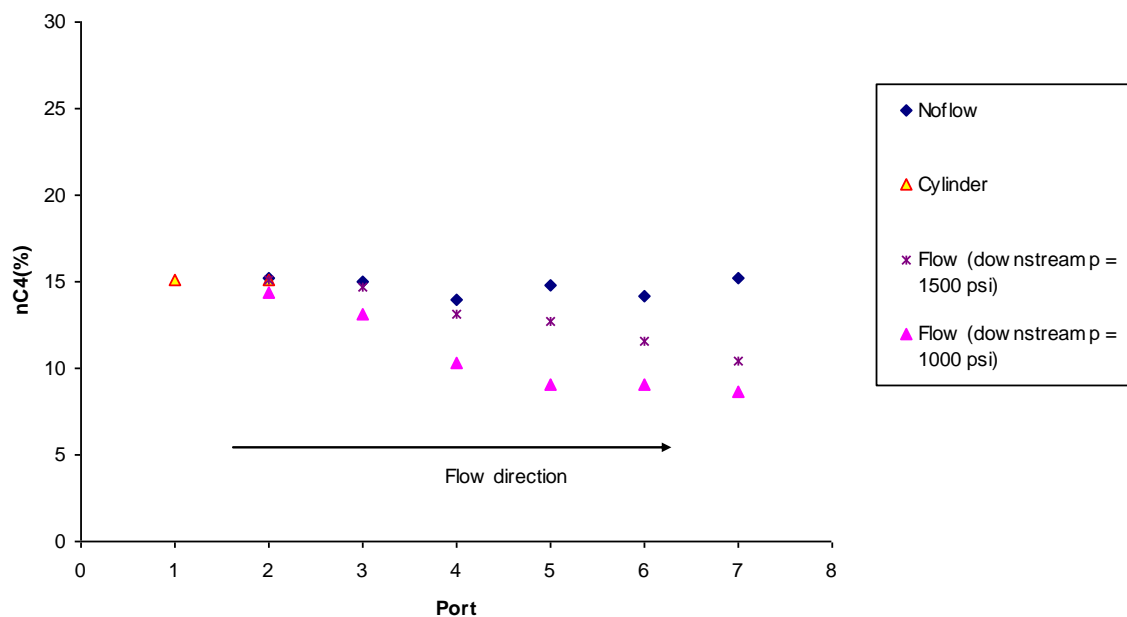


Figure 2-9: Gas-condensate noncapture experiment: nC_4 in the flowing mixture with different BHP control cases.

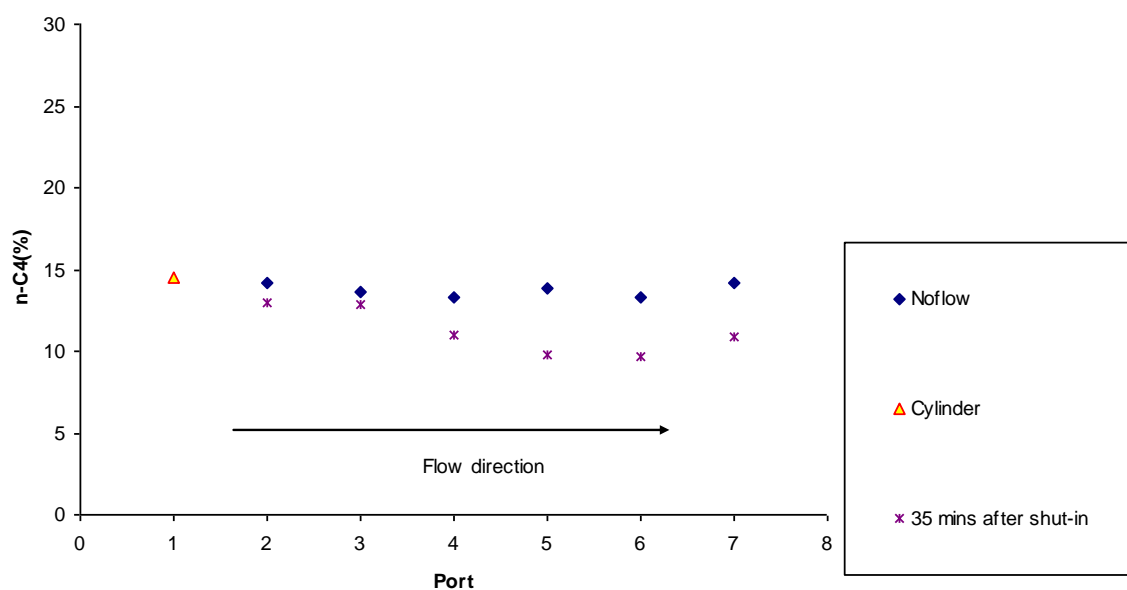


Figure 2-10: Condensate revaporization after noncapture experiment for gas-condensate system 1.

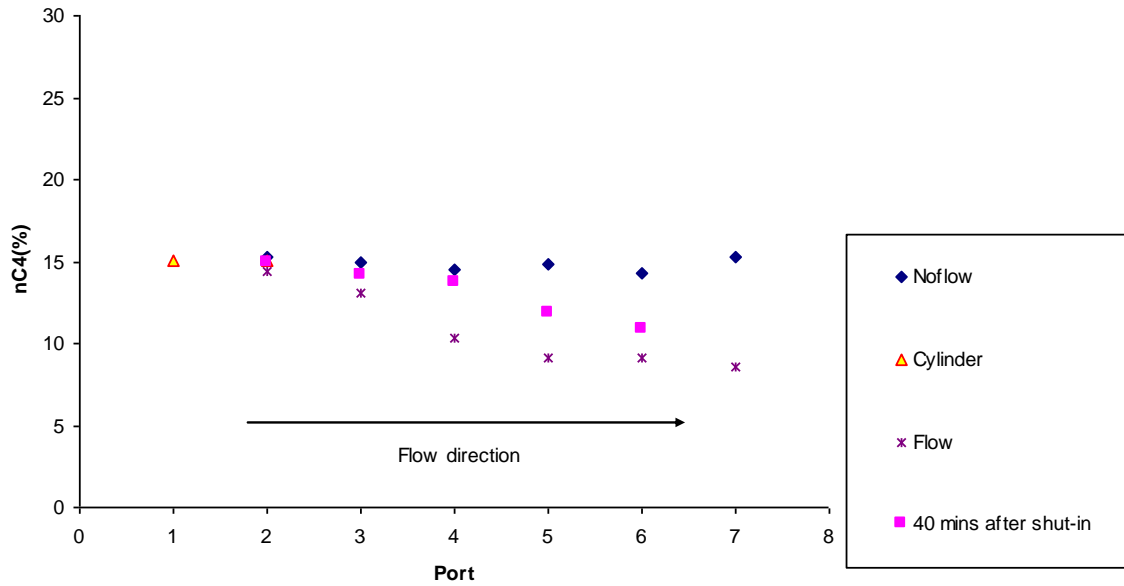


Figure 2-11: Condensate revaporization after noncapture experiment for gas-condensate system 2.

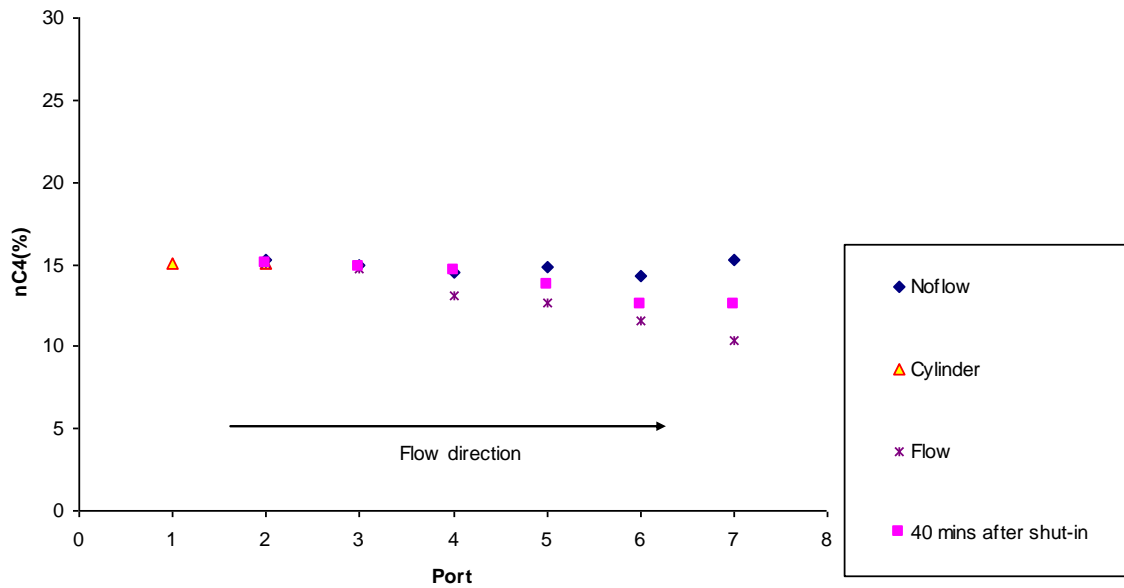


Figure 2-12: Condensate revaporization after noncapture experiment for gas-condensate system 3.

Capture Experiments

The results of a capture experiment are shown in Figure 2-13. Good repeatability was achieved under both static conditions and flowing conditions. The compositional distribution along the core shows a similar trend of liquid dropout as the trend seen during noncapture experiments. A second capture experiment also confirmed the result (Figure 2-14).

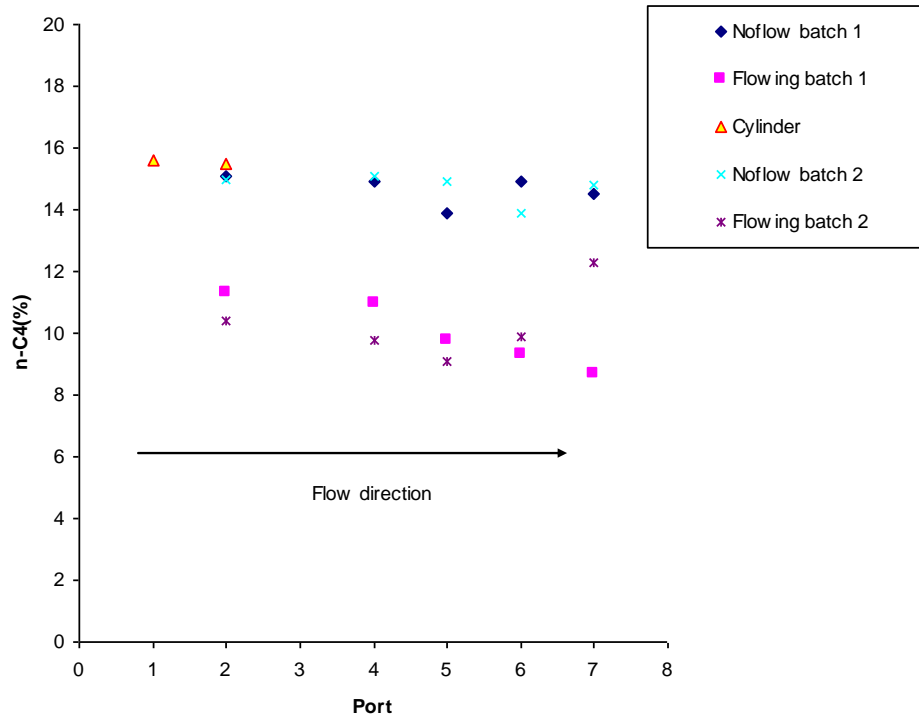


Figure 2-13: Gas-condensate capture experiment 1.

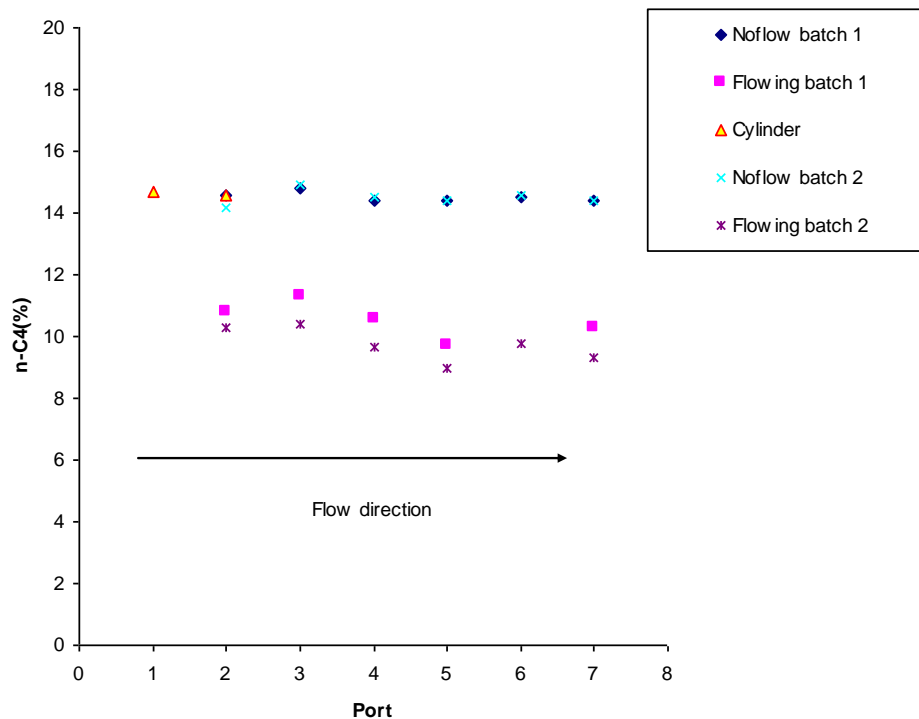


Figure 2-14: Gas-condensate capture experiment 2.

Figure 2-15 shows the result of another capture experiment. However in this case, after taking samples in the capture mode, we discharged all gas and condensate into a vacuumed empty cylinder. When the core and discharge cylinder reached pressure

equilibrium (at low pressure), we disconnected the core from the cylinder and took samples from each of them. The nC_4 compositions in the discharge cylinder and core were very high, which confirmed that the liquid condensate that had deposited in the core was rich in nC_4 .

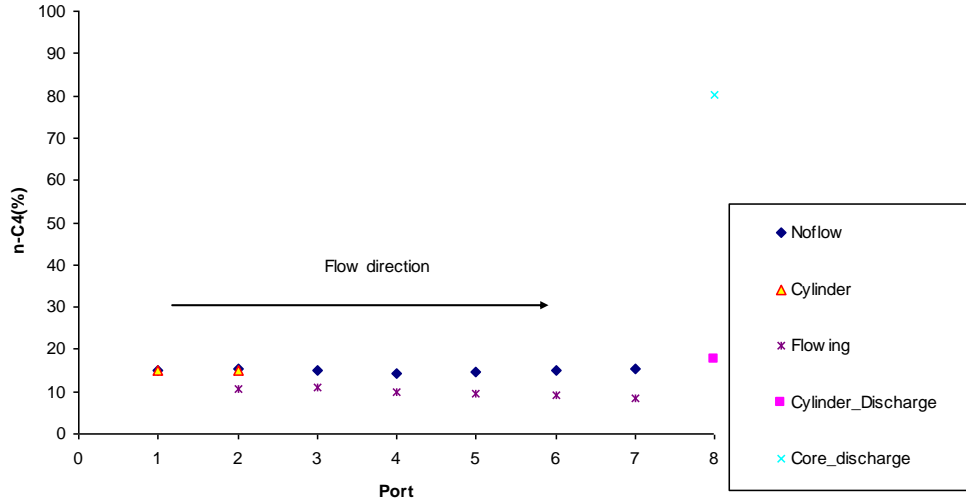


Figure 2-15: Gas-condensate capture experiment 3.

2.4.2. Gas-Condensate with Immobile Water

Comparing Figures 2-6 to 2-12 (without water in the core) to Figures 2-16 and Figure 2-17 for the system with immobile water in the core, it is clear that in the presence of immobile water, condensate still dropped out in the core. The higher the pressure drop, the more liquid dropped out in the core and accumulated in the rock. The flowing mixture became lighter (more C_1) and the concentration of nC_4 in the flowing phase decreased.

The presence of the immobile water did not seem to alter the flow or composition behavior in comparison to experiments in which no water was present.

2.5. Saturation

Figure 2-18 shows condensate saturation distribution calculated from CT scanning. Slice #1 is on the upstream of P_2 , slice #2 is between P_1 and P_2 , etc., and slices #7 and #8 are on the downstream of P_7 . The condensate saturation profile is consistent with the nC_4 compositional profile, although the saturation value estimated at slice #8 appears to be influenced by end-effect. It should be noted that due to the low porosity rock, there is only a small density difference between the liquid n -butane and methane, so the difference between CT numbers of C_1 - nC_4 mixture saturated, C_1 -saturated and nC_4 -saturated rock is not large. This limits the accuracy of the saturation estimation.

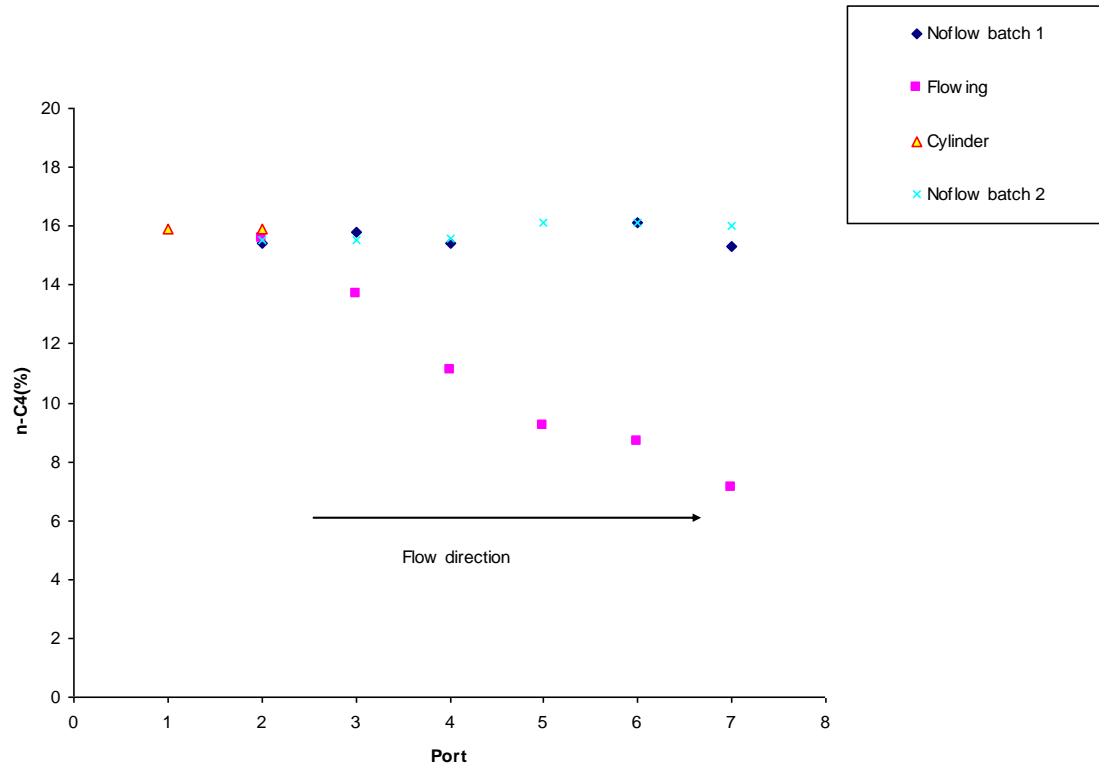


Figure 2-16: Gas-condensate-immobile water noncapture experiment 1: $n\text{C}_4$ in the flowing mixture.

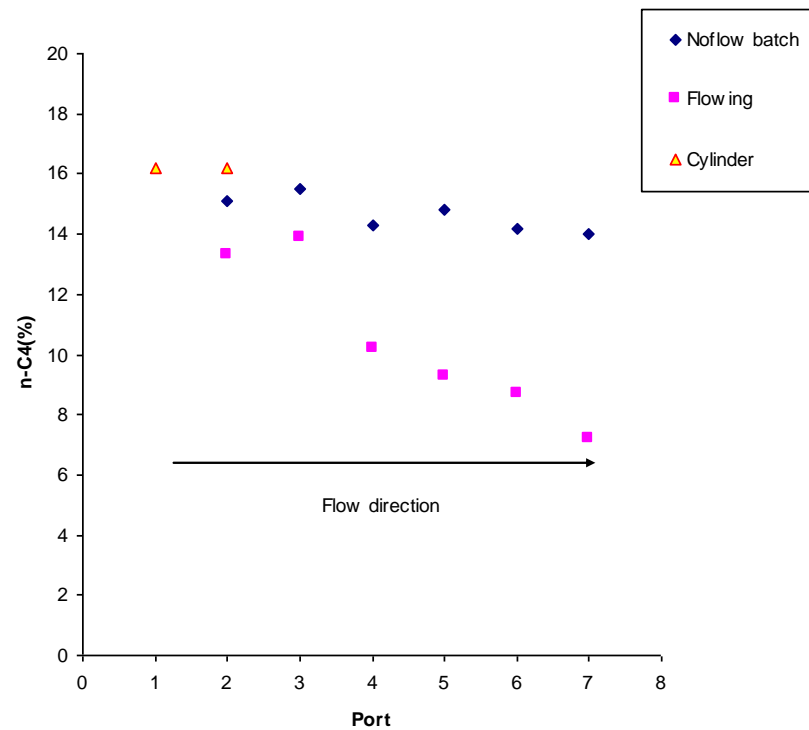
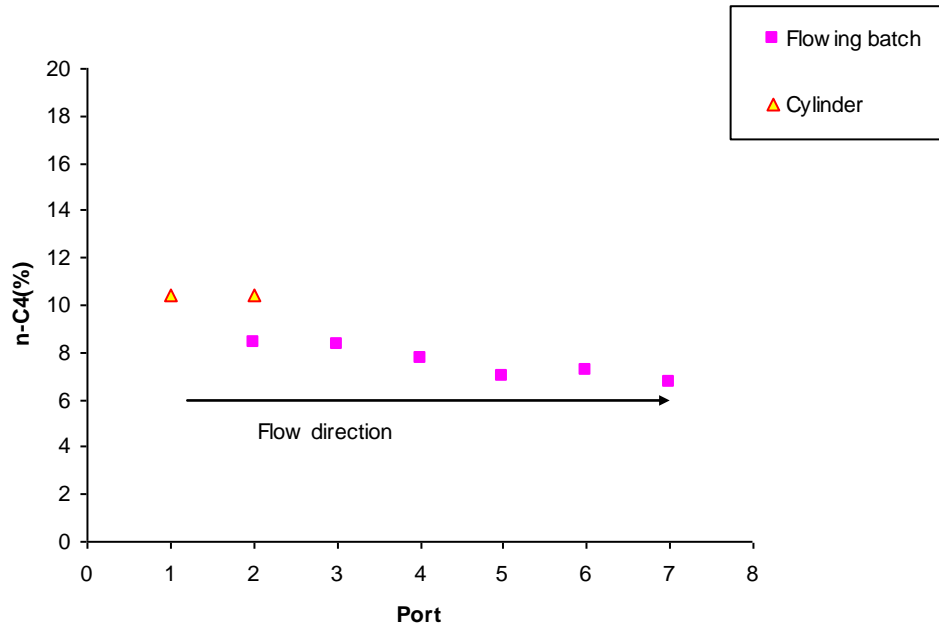
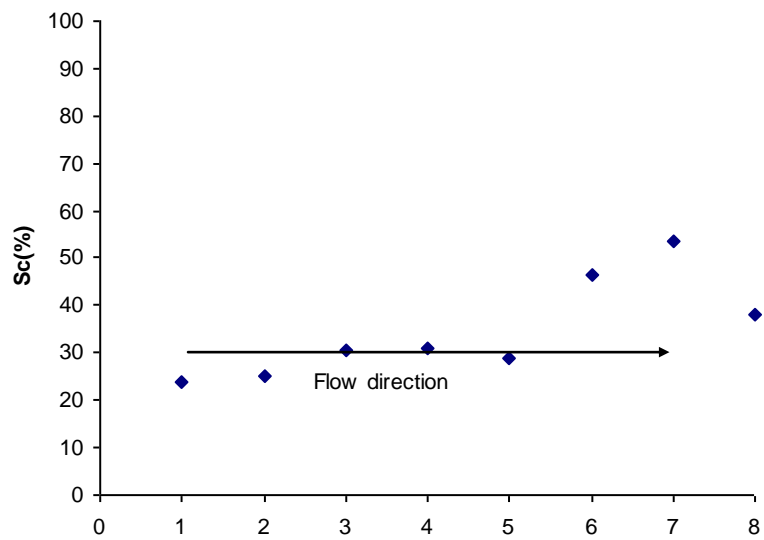


Figure 2-17: Gas-condensate-immobile water noncapture experiment 2: $n\text{C}_4$ in the flowing mixture.



(a)



(b)

Figure 2-18: Gas-condensate noncapture experiment 3: (a) nC_4 in the flowing phases. (b) condensate saturation profile.

3. Impact to Producers

3.1. Optimization of Revenue from Gas-Condensate Reservoirs

As an example of the impact of the change in composition on production from real gas-condensate reservoirs, we will show an example in which the revenue stream was optimized by capitalizing on the variation of condensate yield caused by the shift in the phase envelope. These results are specific to the (hypothetical) example reservoir simulated, and therefore are not necessarily general. Nonetheless, the approach illustrated here can be applied to actual reservoirs by replicating this approach, but using the simulation model of the reservoir under investigation. The model results shown here for demonstration indicate the validity of the concept of taking advantage of the knowledge of the composition change during production, by implementing a production/injection strategy that adjusts the resulting fluid compositions in the reservoir.

In the example case, the model we used is based on the *SPE3* model (Kenyon and Behie, 1987) used for the Third SPE Comparative Solution Project on Gas Cycling of Retrograde Condensate Reservoirs, as shown in Figure 3-1. This model was chosen for this illustrative case, as it represents an industry-standard example. The simulation grid has $9 \times 9 \times 4$ blocks in Cartesian coordinates. There are four layers and only one production well at the center of the reservoir which is perforated in layers 3 and 4. The reservoir fluid is gas-condensate with multiple components. Figure 3-2 shows the phase diagram of the reservoir fluid, which has the composition shown in Table 3-1. At the reservoir temperature of $200^\circ F$, there is a large condensate region between 3500 psia and 500 psia (reservoir pressure is 3500 psia). The initial conditions for the location of the gas/water contact and the capillary pressure data generate a water/gas transition zone extending into the pay layers.

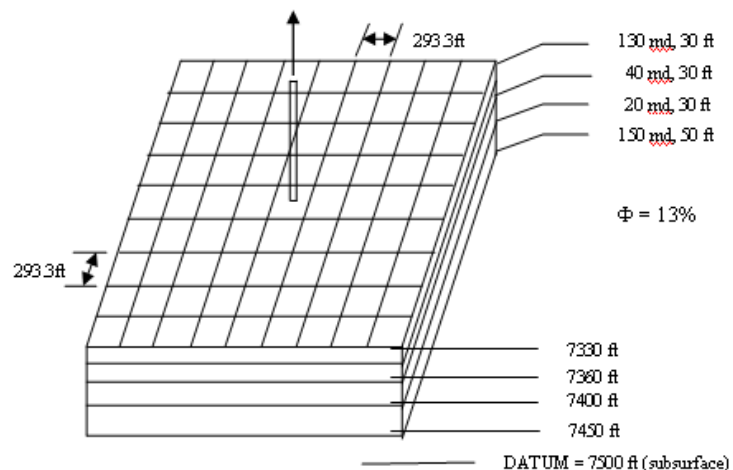


Figure 3-1: The SPE3 reservoir model (Kenyon and Behie, 1987).

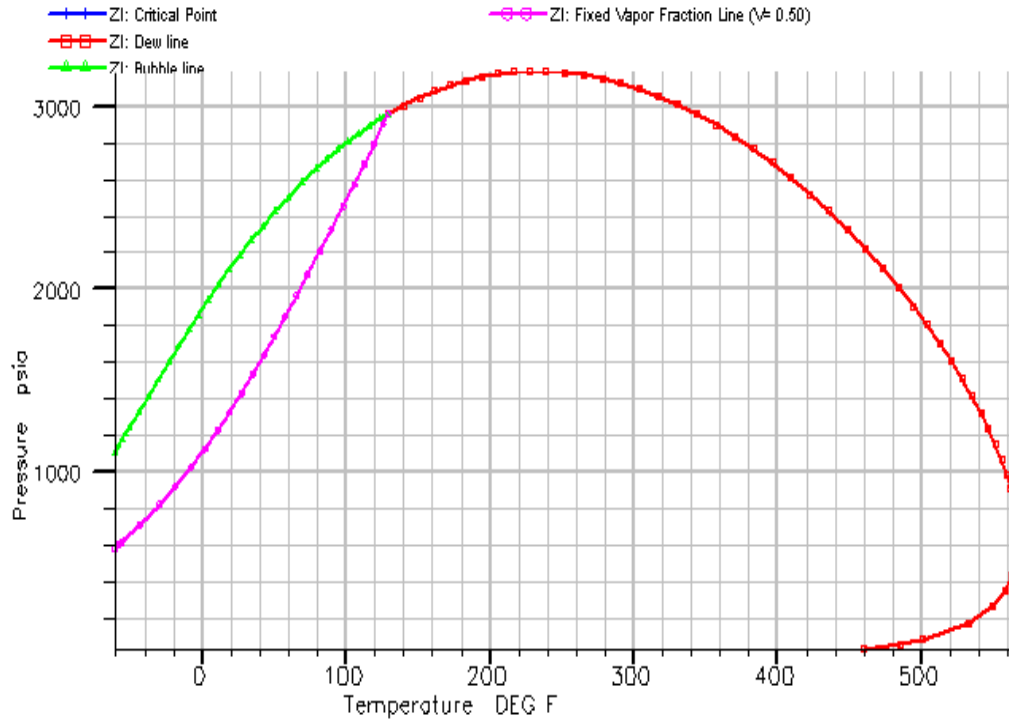


Figure 3-2: Phase diagram of the gas-condensate reservoir fluid.

Table 3-1: Composition of fluid in SPE3 reservoir model.

	z	MW
CO ₂	0.0121	44.01
N ₂	0.0194	28.01
C ₁	0.6599	16.04
C ₂	0.0869	30.07
C ₃	0.0591	44.10
C ₄₋₆	0.0967	66.87
C ₇₊₁	0.0475	107.78
C ₇₊₂	0.0152	198.56
C ₇₊₃	0.0033	335.20

In the optimization problem we modified the SPE3 reservoir problem by considering C₁ injection. The SPE3 model was augmented in this case to have one injector and two producers. The two producers are set at a constant gas production rate of 4,500 Mscf/d. The gas injection rate is varied to achieve the maximum net present value NPV. The objective function is:

$$\text{NPV} = \text{FOPT} \times 80 + \text{FGPT} \times 4 - \text{FGIT} \times 6. \quad (3.1)$$

FOPT: Field Oil Production Total (STB)

FGPT: Field Gas Production Total (Mscf)

FGIT: Field Gas Injection Total (Mscf).

In this calculation, the discount factor was taken to be zero. 80 is the oil price (\$/STB), 4 is the produced gas price (\$/Mscf), and 6 is the cost for injecting gas (\$/Mscf).

The optimization algorithm used was gradient-based. This is likely to be the most suitable kind of algorithm for producers to use in optimizing field problems involving gas-condensate reservoirs. For the compositional problem of gas-condensate in a large and complex reservoir, gradient-based algorithms are preferred because of the computational cost of the simulation runs (function evaluations). The difficulty with a gradient-based algorithm is to calculate gradients of the objective function with respect to the control parameters. This requires either access to the source code or a simulator that has the gradient based optimization capabilities built-in. In the study, we used the commercial compositional simulator ECLIPSE 300.

Figure 3-3 shows the result found to be optimal in terms of NPV for this example problem. Figures 3-4 to 3-6 show the monetary outcome as well as the liquid and gas production as a function of time. In this example case, the optimal result is not the one with maximum sustained injection rate or even the maximum cumulative injection (Figure 3-7). It is evident that injecting C_1 changes the thermodynamic properties of the fluid system, increasing the liquid yield as shown in the liquid/gas ratio in Figure 3-8. This emphasizes the results of the research, namely that the change of composition during production (and injection) influences the optimal strategy.

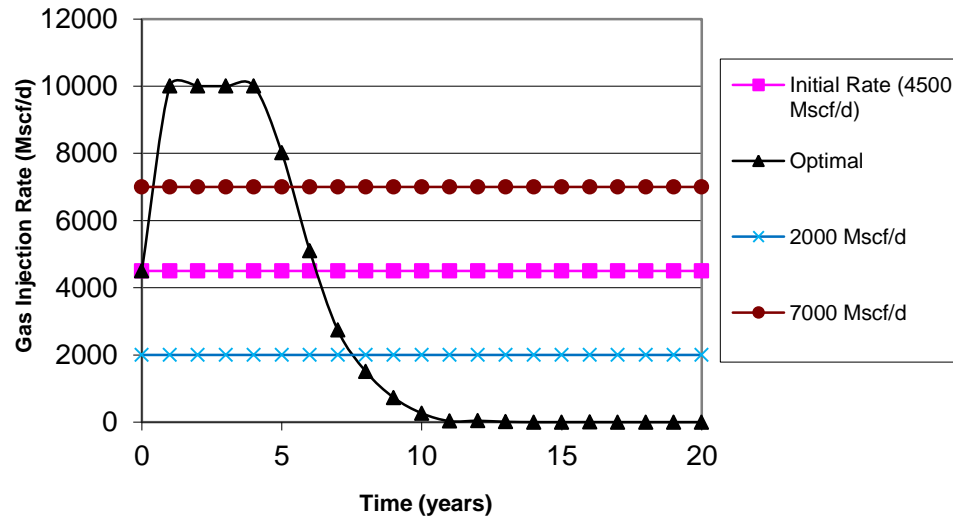


Figure 3-3: Gas injection rate of the optimization problem.

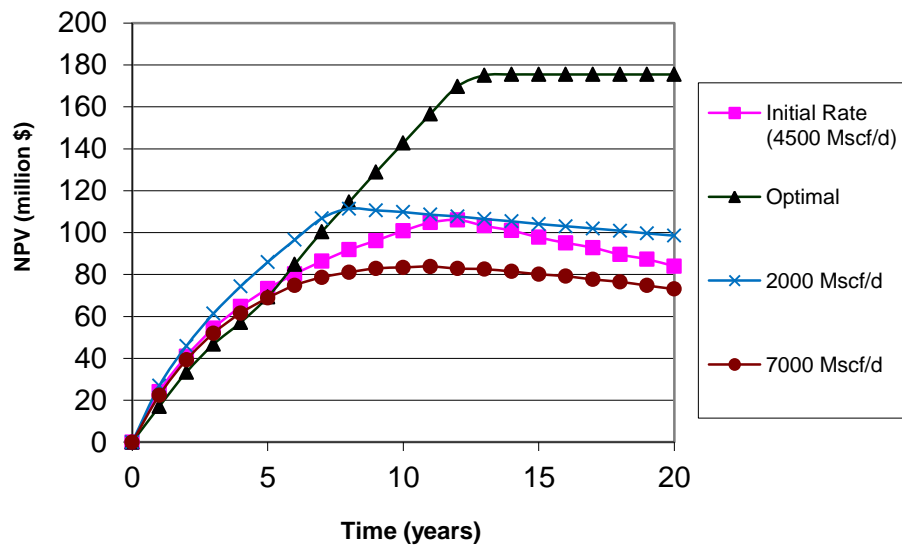


Figure 3-4: Revenue of an example gas-condensate reservoir under different injection rate scenarios.

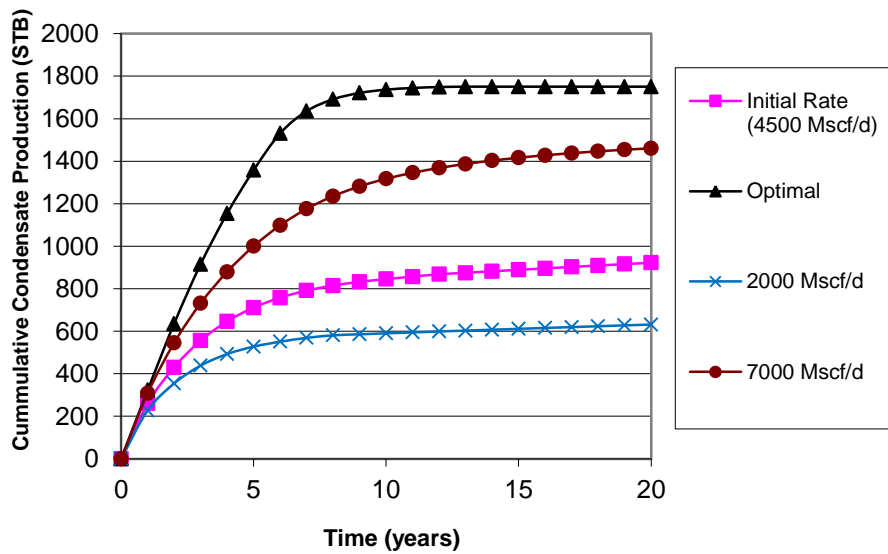


Figure 3-5: Cumulative condensate production of the optimization problem.

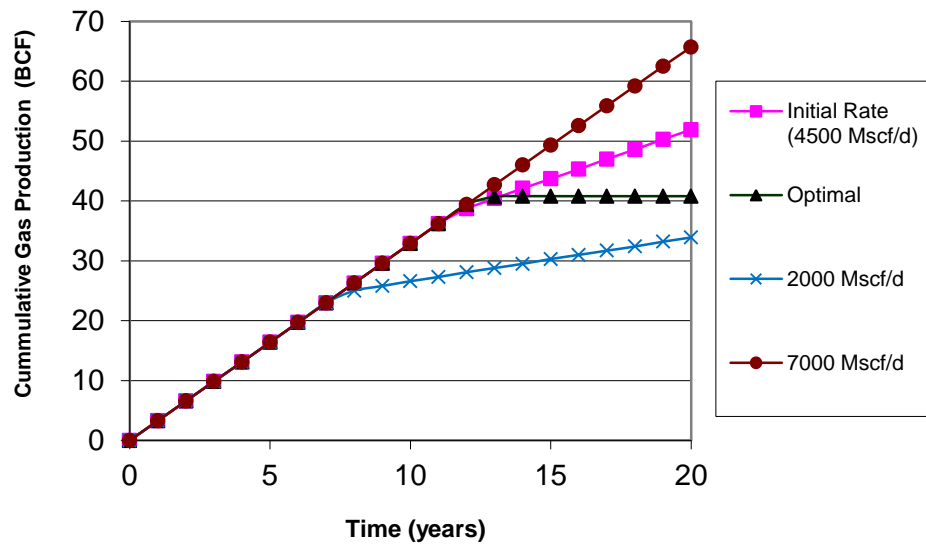


Figure 3-6: Cumulative gas production of the optimization problem.

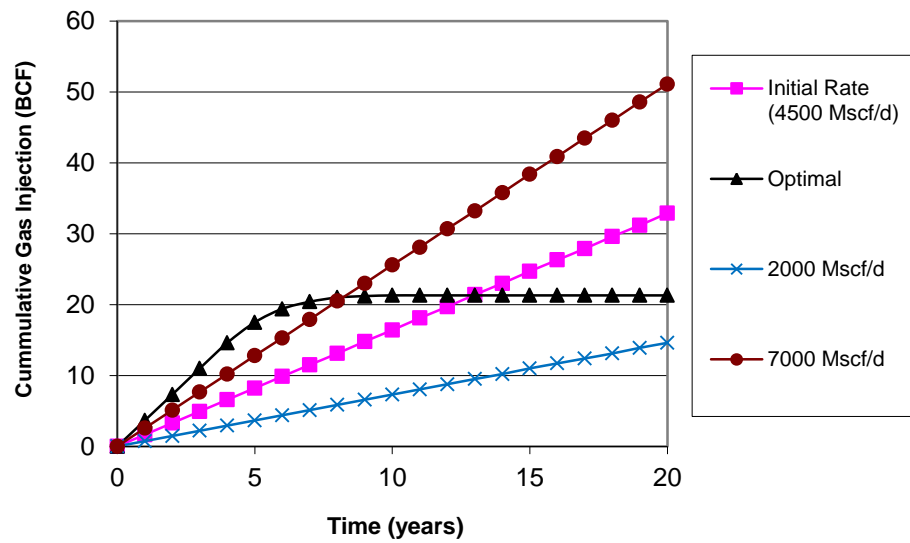


Figure 3-7: Cumulative gas injection of the optimization problem.

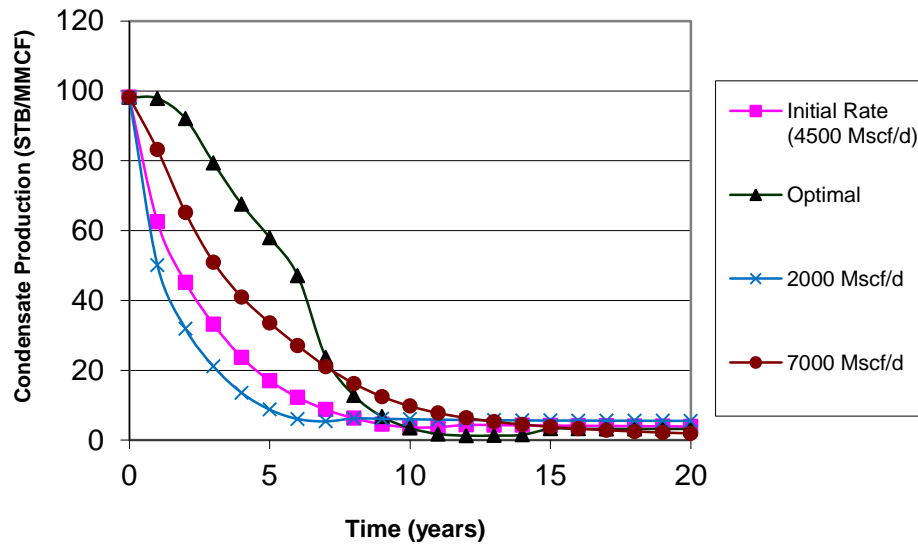


Figure 3-8: Condensate to gas production ratio of the optimization problem.

These results are specific to the (hypothetical) reservoir simulated in the problem, and therefore are not necessarily general. Nonetheless, the optimization illustrated here can be applied to actual reservoirs by replicating this approach, but using the simulation model of the reservoir under investigation. The model results shown here for demonstration indicate the validity of the concept of taking advantage of the knowledge of the composition change during production, by implementing a production/injection strategy that adjusts the resulting fluid compositions in the reservoir to minimize the impact of condensate dropout.

4. Conclusion

The main conclusions of this study are:

- Repeatability of the experiments was achieved, demonstrating the validity of the results.
- Due to the relative permeability and the consequent difference in mobilities of gas and condensate phase, the local composition will change hence the phase envelope of the mixture will shift from a gas-condensate to a volatile oil. This shift was evident in both the experiments and the simulation results, as the thermodynamic behavior followed a different phase envelope during production than that of the original fluid.
- Condensate banking still occurs in the presence of immobile water. Water did not have any measurable effect on the compositional variation of the gas condensate in the experiments done here.
- Shutting a well to remove the condensate banking may not be a useful strategy as the condensate may not be able to revaporize due to the shift of the phase envelope.
- Condensate banking can be reduced by minimizing the pressure drop below the dew point, either by producing the well slowly or by applying partial pressure maintenance using gas injection.
- The performance of a gas condensate well can be improved by using a proper production strategy. The procedures by which this improvement can be achieved were determined in this work, and would take the form of an optimization algorithm applied to the numerical reservoir model of the field under consideration.

References

- Afidick, D., Kaczorowski, N.J., and Bette, S., 1994, “*Production Performance of a Retrograde Gas Reservoir: A Case Study of the Arun Field*”, Presentation at SPE Asia Pacific Oil and Gas Conference, Melbourne, Australia, SPE 28749.
- Barnum, R.S., Brinkman, F.P., Richardson, T.W., and Spillette, A.G., 1995, “*Gas Condensate Reservoir Behavior: Productivity and Recovery Reduction Due to Condensation*”, Presentation at SPE Annual Technical Conference and Exhibition, Dallas, USA, SPE 30767.
- Kenyon, D. E., Behie, G. A., 1987, “Third SPE Comparative Solution Project: Gas Cycling of Retrograde Condensate Reservoirs”. *Journal of Petroleum Technology*, August 1987.
- Shi, Chunmei, 2009, “*Flow Behaviors of Gas Condensate Wells*”, Ph.D. Dissertation, Stanford University, California.